Design of Self-supporting Surfaces
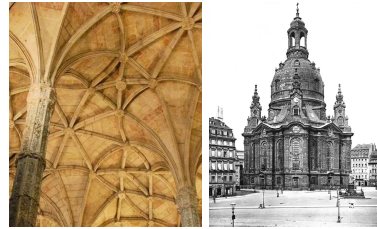
Abstract

todo

Figure 1: *Nonconvex self-supporting masonry. Left: vaults of a gothic cathedral; Right: dome of Frauenkirche, Dresden*
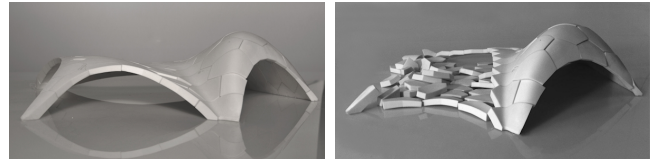

Figure 2: *Freeform masonry vault (left) and failure of the same (right). These are mock-up models from the Block Research Group at ETH Zürich.*

1 Introduction

TODO gentle introduction to self-supporting surfaces, assumptions about the model, importance to architecture etc

Vaulted masonry structures are among the simplest and at the same time most elegant solutions for creating curved shapes in building construction. This is the reason why they have been an object of interest since antiquity, and why they continue to be an active topic of research in today's engineering community. The shapes range from convex to non-convex to freeform (see Figures 1 and 2).

Our paper is concerned with a combined geometry+statics analysis of *self-supporting* masonry and with tools for the interactive modeling of freeform self-supporting structures. Here 'self-supporting' means that the structure, considered as an arrangement of blocks (bricks, stones), holds together by itself, and additional support, additional chains and similar are present only during construction. Our analysis is based on the following assumptions, which follow the classic [Heyman 1966]:

Assumption 1: Masonry has no tensile strength, but the individual building blocks do not slip against each other (because of friction or mortar). On the other hand, their compressive strength is sufficiently high so that failure of the structure is by a sudden change in geometry, such as shown by Figure 2, and not by material failure.

Assumption 2 (the Safe Theorem): If a system of forces can be found which is in equilibrium with the load on the structure and which is contained within the masonry envelope then the structure will carry the loads, although the actually occurring forces may not be those postulated.

Our approach is twofold: We first investigate the continuous case of a smooth surface under stress which turns out to be governed by the so-called *Airy stress function*. This mathematical model is called a *membrane* in the engineering literature and has been applied to the analysis of masonry before. The surface is self-supporting if and only if stresses are entirely compressive (i.e., the Airy function is convex).

For computational purposes, stresses are discretized as a fictitious *thrust network* contained in the masonry structure. This is a system of forces which together with the structure's deadload is in equilibrium. It can be interpreted as a finite element discretization of continuous case, and it turns out to have very interesting geometry: we have a polyhedral Airy stress function and a reciprocal force diagram, both of which are present in earlier work. Our own contributions are the following:

Contributions.

• We connect the physics of self-supporting surfaces with vertical loads to the geometry of isotropic 3-space, whith the direction of gravity as the distinguished direction (§2.3). Taking the convex Airy potential as unit sphere, one can express the equations (1) governing self-supporting surfaces in terms of curvatures.

• We employ Maxwell's construction of polyhedral thrust networks and their reciprocal diagrams (§2.4), and give an interpretation of the equilibrium conditions in terms of discrete curvatures.

- The graph Laplacian derived from a thrust network with compressive forces is a 'perfect' one. We show how it appears in the analysis and establish a connection with mean curvatures which are otherwise defined for polyhedral surfaces.

- We present an optimization algorithm for efficiently finding a thrust network near a given arbitrary reference surface (§3), and build a tool for interactive design of self-supporting surfaces based on this algorithm (§4).

- We exploit the geometric relationships between a self-supporting surface and the 'unit sphere' stress potential in order to find particularly nice families of self-supporting surfaces, especially planar quadrilateral representations of thrust networks (§5).

- We demonstrate the versatility and applicability of our approach to the design and analysis of large-scale masonry and steel-glass structures.

Related Work. Unsupported masonry has been an active topic of research in the engineering community. The foundations for the modern approach were laid by Jacques Heyman [1966] and are available as the textbook [Heyman 1995]. A unifying view on polyhedral surfaces, compressive forces and corresponding 'convex' force diagrams is presented by [Ash et al. 1988]. F. Fraternali [2002], [2010] established a connection between the continuous theory of stresses in membranes and the discrete theory of forces in thrust networks, by interpreting the latter as a non-conforming finite element discretization of the former.

Several authors have studied the problem of finding discrete compressive force networks contained within the boundary of masonry structures; early work in this area includes [Schek 1974], [Livesley 1992], and [O'Dwyer 1998]. Fraternali [2010] proposed solving for the structure's discrete stress surface, and examining its convex hull to study the structure's stability and susceptibility to cracking. Philippe Block's seminal thesis [2007] introduced the method of Thrust Network Analysis, which linearizes the form-finding problem by first seeking a reciprocal diagram of the top view, which guarantees equilibrium of horizontal forces, then solving for the heights that balance the vertical loads. Recent work by Block and coauthors extend this method in the case where the reciprocal diagram is not unique; for different choices of reciprocal diagram, the optimal heights can be found using the method of least squares [Van Mele and Block 2011], and the search for the best such reciprocal diagram can be automated using a genetic algorithm [Block and Lachauer 2011].

Other approaches to the interactive design of self-supporting structures include modeling these structures as damped particle-spring systems [Kilian and Ochsendorf 2005; Barnes 2009], mirroring the rich tradition in architecture of designing self-supporting surfaces using hanging chain models [Heyman 1998]. Alternatively, masonry structures can be represented by networks of rigid blocks [Whiting et al. 2009], whose conditions on the structural feasibility were incorporating into procedural modeling of buildings.

Algorithmic and mathematical methods relevant to this paper are work on the geometry of quad meshes with planar faces ([Glymph et al. 2004], [Liu et al. 2006]), discrete curvatures for such meshes [Pottmann et al. 2007], in particular curvatures in isotropic geometry [Pottmann and Liu 2007]. Schiftner and Balzer [2010] discuss approximating a reference surface by quad mesh with planar faces, whose layout is guided by statics properties of that surface.
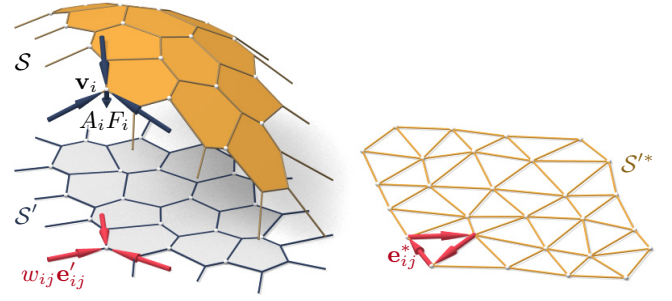

Figure 3: *Self-supporting thrust network $\mathcal{S}$, dangling edges indicating the directions of external forces (left). This network together with compressive forces which balance vertical loads "$A_i F_i$" projects onto a planar mesh $\mathcal{S}'$ with equilibrium compressive forces "$w_{ij} \mathbf{e}'_{ij}$" in its edges. Rotating forces by 90 degrees leads to the reciprocal force diagram $\mathcal{S}'^*$ (right).*

2 Self-supporting Surfaces

2.1 The Continuous Theory

We are here modeling masonry as a surface S given by a height field $s(x, y)$ defined in some planar domain Ω. We assume that there are vertical loads $F(x, y)$ — usually F represents the structure's own weight. By definition this surface is self-supporting, if and only if there exists a field of compressive stresses which are in equilibrium with the acting forces. This is equivalent to existence of a field $M(x, y)$ of 2×2 symmetric positive semidefinite matrices satisfying

$$\operatorname{div}(M \nabla s) = F, \quad \operatorname{div} M = 0, \tag{1}$$

where the divergence operator $\operatorname{div}\begin{pmatrix} u(x,y) \\ v(x,y) \end{pmatrix} = u_x + v_y$ is understood to act on the columns of a matrix (see e.g. [Fraternali 2010], [Giaquinta and Giusti 1985]).

The condition $\operatorname{div} M = 0$ says that M is essentially the Hessian of a real-valued function ϕ (the *Airy stress potential*): With the notation

$$M = \begin{pmatrix} m_{11} & m_{12} \\ m_{12} & m_{22} \end{pmatrix} \iff \widehat{M} = \begin{pmatrix} m_{22} & -m_{12} \\ -m_{12} & m_{11} \end{pmatrix}$$

it is clear that $\operatorname{div} M = 0$ is an integrability condition for $\widehat{M}$, so locally there is a potential ϕ with

$$\widehat{M} = \nabla^2 \phi, \quad \text{i.e.,} \quad M = \widehat{\nabla^2 \phi}.$$

If the domain Ω is simply connected, this relation holds globally. Positive semidefiniteness of M (or equivalently of $\widehat{M}$) then characterizes *convexity* of the Airy potential ϕ.

Remark: Note that $\operatorname{div} M = 0$ yields $\operatorname{div}(M \nabla s) = \operatorname{tr}(M \nabla^2 s)$, which we like to call $\Delta_\phi s$. The operator Δ_ϕ is symmetric, and it is elliptic (as a Laplace operator should be) if and only if M is positive definite, i.e., ϕ is strictly convex. The balance condition (1) may be written as $\Delta_\phi s = F$.

Remark: Stresses at boundary points depend on the way the surface is anchored: A fixed anchor means no condition, but a free boundary with outer normal vector $\mathbf{n}$ means $\langle M \nabla s, \mathbf{n} \rangle = 0$.

2.2 Discrete Theory: Thrust Networks

We are now going to discretize a self-supporting surface by a polyhedral mesh $\mathcal{S} = (V, E, F)$ (see Figure 3). Loads are again vertical, and we discretize them as force densities F_i associated with

vertices $\mathbf{v}_i$. The load acting on this vertex is then given by $F_i A_i$, where A_i is an area of influence (using a prime to indicate projection onto the xy plane, A_i is the area of the Voronoi cell of $\mathbf{v}'_i$ w.r.t. V'). We assume that stresses are carried by the edges of the mesh: the force exerted on the vertex $\mathbf{v}_i$ by the edge connecting $\mathbf{v}_i, \mathbf{v}_j$ is given by

$$w_{ij}(\mathbf{v}_j - \mathbf{v}_i), \quad \text{where} \quad w_{ij} = w_{ji} \geq 0.$$

The nonnegativity of the individual weights w_{ij} expresses the compressive nature of forces. The balance conditions at vertices then read as follows: With $\mathbf{v}_i = (x_i, y_i, s_i)$ we have

$$\sum_{j \sim i} w_{ij}(x_j - x_i) = \sum_{j \sim i} w_{ij}(y_j - y_i) = 0, \quad (2)$$

$$\sum_{j \sim i} w_{ij}(s_j - s_i) = A_i F_i. \quad (3)$$

A mesh equipped with edge weights in this way is a discrete *thrust network*. Invoking the safe theorem, we can state that a masonry structure is self-supporting, if we can find a thrust network with compressive forces which is entirely contained within the structure.

Reciprocal Diagram. Equations (2) have a geometric interpretation: With edge vectors

$$\mathbf{e}'_{ij} = \mathbf{v}'_j - \mathbf{v}'_i = (x_j, y_j) - (x_i, y_i),$$

(2) asserts that vectors $w_{ij}\mathbf{e}'_{ij}$ form a closed cycle. Rotating them by 90 degrees, we see that likewise

$$\mathbf{e}'^{*}_{ij} = w_{ij} J \mathbf{e}'_{ij}, \quad \text{with} \quad J = \begin{pmatrix} 0 & -1 \\ 1 & 0 \end{pmatrix}.$$

form a closed cycle (see Figure 3). If the mesh $\mathcal{S}$ is simply connected, there exists an entire *reciprocal diagram* $\mathcal{S}'^{*}$ which is a combinatorial dual of $\mathcal{S}$, and which has edge vectors $\mathbf{e}'^{*}_{ij}$. Its vertices are denoted by $\mathbf{v}'^{*}_i$.

Polyhedral Stress Potential. We can go further and construct a convex polyhedral surface Φ with vertices $\mathbf{w}_i = (x_i, y_i, \phi_i)$ combinatorially equivalent to $\mathcal{S}$ by requiring that a primal face of Φ lies in the plane $z = \alpha x + \beta y + \gamma$ if and only if (α, β) is the corresponding dual vertex of $\mathcal{S}'^{*}$ (see Figure 4). Obviously this condition determines Φ up to vertical translation. For existence see [Ash et al. 1988]. The inverse procedure constructs a reciprocal diagram from Φ. This procedure obviously works also if forces are not compressive: we can construct an Airy mesh Φ which has planar faces, but it will no longer be a convex polyhedron.

The vertices of Φ can be interpolated by a piecewise-linear function $\phi(x, y)$. It is easy to see that the derivative of $\phi(x, y)$ jumps by the amount $\|\mathbf{e}'^{*}_{ij}\| = w_{ij}\|\mathbf{e}'_{ij}\|$, when crossing over the edge $\mathbf{e}'_{ij}$ at right angle, with unit speed. This identifies Φ as the Airy polyhedron introduced by [Fraternali et al. 2002] as a finite element discretization of the continuous Airy function (see also [Fraternali 2010]).

Polarity. Polarity with respect to the *Maxwell paraboloid* $z = \frac{1}{2}(x^2 + y^2)$ maps the plane $z = \alpha x + \beta y + \gamma$ to the point $(\alpha, \beta, -\gamma)$. Thus, applying polarity to Φ and projecting the result Φ^{*} into the xy plane reconstructs the reciprocal diagram $\Phi^{*'} = \mathcal{S}'^{*}$ (see Fig. 4).

Remark: The edge weights w_{ij} may be used to define a graph Laplacian Δ_ϕ which acts on a vertex-based function s by $\Delta_\phi s(\mathbf{v}_i) = \sum_{j \sim i} w_{ij}(s_j - s_i)$. It is symmetric and semidefinite. Equation (2) directly implies linear precision for the planar 'top view mesh' $\mathcal{S}'$ (i.e., $\Delta_\phi f = 0$ if f is a linear function). Furthermore, Δ_ϕ-harmonic functions enjoy a maximum principle. Equation (3) can be written as $\Delta_\phi s = AF$.
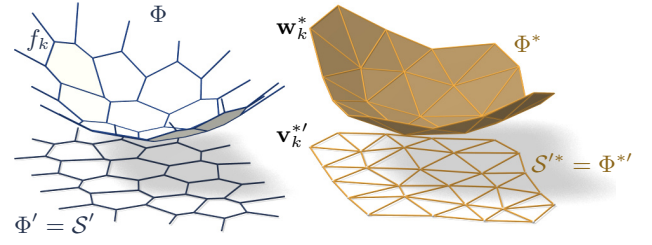

Figure 4: *Airy stress potential Φ and its polar dual Φ^{*}. Φ projects onto the same planar mesh as $\mathcal{S}$ does, while Φ^{*} projects onto the reciprocal force diagram. A primal face f_k lies in the plane $z = \alpha x + \beta y + \gamma \iff$ the corresponding dual vertex is $\mathbf{w}^{*}_k = (\alpha, \beta, -\gamma)$.*

2.3 Surfaces in Isotropic Geometry

It is worth wile to reconsider the basics of self-supporting surfaces in the language of dual-isotropic geometry, which takes place in $\mathbb{R}^3$ with the z axis as a distinguished vertical direction. The basic elements of this geometry are planes, having equation $z = f(x, y) = \alpha x + \beta y + \gamma$. The gradient vector $\nabla f = (\alpha, \beta)$ determines the plane up to translation. A plane tangent to the graph of the function $s(x, y)$ has gradient vector ∇s.

There is the notion of *parallel points*: $(x, y, z) \parallel (x', y', z') \iff x = x', y = y'$.

In the differential geometry of surfaces one considers the *Gauss map* σ from a surface S to a convex gauge body Φ by requiring that corresponding points have parallel tangent planes. Subsequently mean curvature H^{rel} and Gaussian curvature K^{rel} *relative to* Φ are computed from the derivative $d\sigma$. Classically Φ is the unit sphere (so that σ maps each point its unit normal vector), leading to the ordinary curvatures H and K.

Computing Curvatures. In our setting, parallelity is a property of *points* rather than lines, and the Gauss map σ goes the other way, mapping the tangent planes of the gauge body $z = \phi(x, y)$ to the corresponding tangent plane of the surface $z = s(x, y)$. If we know which point a plane is attached to, then it is determined by its gradient. So we simply write

$$\nabla \phi \overset{\sigma}{\longmapsto} \nabla s.$$

By moving along a curve $\mathbf{u}(t) = (x(t), y(t))$ in the parameter domain we get the first variation of tangent planes: $\frac{d}{dt}\nabla\phi|_{\mathbf{u}(t)} = (\nabla^2\phi)\dot{\mathbf{u}}$. This yields the derivative $(\nabla^2\phi)\dot{\mathbf{u}} \overset{d\sigma}{\longmapsto} (\nabla^2 s)\dot{\mathbf{u}}$, for all $\dot{\mathbf{u}}$, and the matrix of $d\sigma$ is found as $(\nabla^2\phi)^{-1}(\nabla^2 s)$. By definition, curvatures of the surface s *relative* to ϕ are found as

$$K^{\mathrm{rel}}_s = \det(d\sigma) = \frac{\det\nabla^2 s}{\det\nabla^2\phi},$$

$$H^{\mathrm{rel}}_s = \tfrac{1}{2}\operatorname{tr}(d\sigma) = \tfrac{1}{2}\operatorname{tr}\left(\frac{M}{\det\nabla^2\phi}\nabla^2 s\right) = \frac{\Delta_\phi s}{2\det\nabla^2\phi}.$$

The Maxwell paraboloid $\phi_0(x, y) = \frac{1}{2}(x^2 + y^2)$ is called the *unit sphere* of isotropic geometry, its Hessian equals E_2. Curvatures relative to that gauge body are not called 'relative'. We get

$$K_s = \det\nabla^2 s, \ H_s = \frac{\Delta s}{2}, \ K^{\mathrm{rel}}_s = \frac{K_s}{K_\phi}, \ H^{\mathrm{rel}}_s = \frac{\Delta_\phi s}{2K_\phi} = \frac{\Delta_\phi s}{\Delta_\phi \phi}$$

(for the last formula we have used $\operatorname{tr}(M\nabla^2\phi) = \operatorname{tr}(E_2) = 2$).

Relation to Self-supporting Surfaces. Applying the definitions above to the convex Airy stress potential ϕ of a self-supporting surface, we rewrite the balance conditions (1) as

$$2K_\phi H_s^{\text{rel}} = F. \qquad (4)$$

Let us draw some conclusions:

- Since $H_\phi^{\text{rel}} = 1$ we see that the load $F_\phi = 2K_\phi$ is admissible for the stress surface $\phi(x, y)$, which is hereby shown as self-supporting. The quotient of admissible loads yields

$$H_s^{\text{rel}} = F/F_\phi. \qquad (5)$$

- If the stress surface coincides with the Maxwell paraboloid, then *constant loads characterize constant mean curvature surfaces*, because we get $K_\phi = 1$ and $H_s = F/2$.
- If s_1, s_2 have the same stress potential ϕ, then $H_{s_1 - s_2}^{\text{rel}} = H_{s_1}^{\text{rel}} - H_{s_2}^{\text{rel}} = 0$, so $s_1 - s_2$ is a 'relative' minimal surface.

2.4 Meshes in Isotropic Geometry

A general theory of curvatures of polyhedral surfaces with respect to a gauge body was proposed by [Pottmann et al. 2007], and its dual complement in isotropic geometry was elaborated by [Pottmann and Liu 2007]. As also illustrated by Figure 5, the mean curvature of a self-supporting surface $\mathcal{S}$ *relative* to its discrete Airy stress potential is associated with the vertices of $\mathcal{S}$. It is computed from areas and mixed areas of faces in the polar polyhedra $\mathcal{S}^*$ and Φ^* which correspond to the vertex $\mathbf{v}_i$:

$$H^{\text{rel}}(\mathbf{v}_i) = \frac{A_i(\mathcal{S}, \Phi)}{A_i(\Phi, \Phi)}, \quad \text{where}$$

$$A_i(\mathcal{S}, \Phi) = \frac{1}{4} \sum_{k:\, f_k \in \text{1-ring}(\mathbf{v}_i)} \det(\mathbf{v}_k'^*, \mathbf{w}_{k+1}'^*) + \det(\mathbf{w}_k'^*, \mathbf{v}_{k+1}'^*).$$

The prime denotes the projection into the xy plane, and summation is over those dual vertices which are adjacent to $\mathbf{v}_i$. Replacing $\mathbf{v}_k^*$ by $\mathbf{w}_k^*$ yields $A_i(\Phi, \Phi) = \frac{1}{2} \sum \det(\mathbf{w}_k'^*, \mathbf{w}_{k+1}'^*)$.
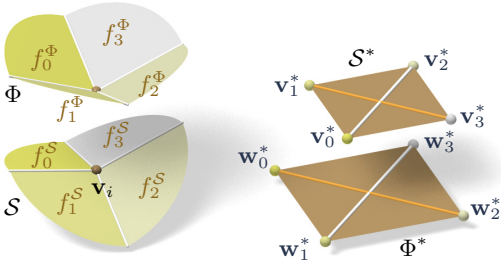

Figure 5: *Mean curvature of a vertex $\mathbf{v}_i$ of $\mathcal{S}$: Corresponding edges of the polar duals $\mathcal{S}^*$, Φ^* are parallel, and mean curvature according to [Pottmann et al. 2007] is computed from the vertices polar to faces adjacent to $\mathbf{v}_i$. For valence 4 vertices the case of zero mean curvature shown here is characterized by parallelity of non-corresponding diagonals of corresponding quads in $\mathcal{S}^*, \Phi^*$.*

Proposition. *If Φ is the Airy surface of a thrust network $\mathcal{S}$, then the mean curvature of $\mathcal{S}$ relative to Φ is computable as*

$$H^{\text{rel}}(\mathbf{v}_i) = \frac{\sum_{j \sim i} w_{ij}(s_j - s_i)}{\sum_{j \sim i} w_{ij}(\phi_j - \phi_i)} = \frac{\Delta_\phi s}{\Delta_\phi \phi}\bigg|_{\mathbf{v}_i}. \qquad (6)$$

This is an immediate consequence of the following

Lemma. $2A_i(\mathcal{S}, \Phi) = \sum_{j \sim i} w_{ij}(s_j - s_i).$

Proof. Consider edges $\mathbf{e}_1', \ldots, \mathbf{e}_n'$ emanating from $\mathbf{v}_i'$, and the dual cycles in $\Phi^{*'}$ and $\mathcal{S}^{*'}$ which without loss of generality are given by vertices $(\mathbf{v}_1^{*'}, \ldots, \mathbf{v}_n^{*'})$ and $(\mathbf{w}_1^{*'}, \ldots, \mathbf{w}_n^{*'})$, respectively. The former has edges $\mathbf{w}_{j+1}'^* - \mathbf{w}_j'^* = w_{ij} J \mathbf{e}_j'$ (indices modulo n).

Without loss of generality $\mathbf{v}_i = 0$, so the vertex $\mathbf{v}_j'^*$ equals the gradient of the linear function $\mathbf{x} \mapsto \langle \mathbf{v}_j'^*, \mathbf{x} \rangle$ defined by the properties $\mathbf{e}_{j-1}' \mapsto s_{j-1} - s_i$, $\mathbf{e}_j' \mapsto s_j - s_i$. Corresponding edge vectors $\mathbf{v}_{j+1}'^* - \mathbf{v}_j'^*$ and $\mathbf{w}_{j+1}'^* - \mathbf{w}_j'^*$ are parallel, because $\langle \mathbf{v}_{j+1}' - \mathbf{v}_j', \mathbf{e}_j' \rangle = (s_j - s_i) - (s_j - s_i) = 0$. Now expand $2A_i(\mathcal{S}, \Phi)$:

$$\frac{1}{2} \sum \det(\mathbf{w}_j'^*, \mathbf{v}_{j+1}') + \det(\mathbf{v}_j', \mathbf{w}_{j+1}'^*)$$
$$= \frac{1}{2} \sum \det(\mathbf{w}_j'^* - \mathbf{w}_{j+1}'^*, \mathbf{v}_{j+1}') + \det(\mathbf{v}_j', \mathbf{w}_{j+1}'^* - \mathbf{w}_j'^*)$$
$$= \frac{1}{2} \sum \det(-w_{ij} J \mathbf{e}_j', \mathbf{v}_{j+1}') + \det(\mathbf{v}_j', w_{ij} J \mathbf{e}_j')$$
$$= \sum \det(\mathbf{v}_j', w_{ij} J \mathbf{e}_j') = \sum w_{ij} \langle \mathbf{v}_j', \mathbf{e}_j' \rangle = \sum w_{ij}(s_j - s_i).$$

Here we have used $\det(\mathbf{a}, J\mathbf{b}) = \langle \mathbf{a}, \mathbf{b} \rangle$. $\qquad \square$

In order to discretize (4), we also need a discrete Gaussian curvature, which is usually defined as a quotient of areas which correspond under the Gauss mapping. We define

$$K_\Phi(\mathbf{v}_i) = \frac{A_i(\Phi, \Phi)}{A_i},$$

where A_i is the Voronoi area of vertex $\mathbf{v}_i'$ in the projected mesh $\mathcal{S}'$, which was used in (3).

Discrete Balance Equation. We now prove the discrete analogue to Equation (4).

Theorem. *A simply-connected mesh $\mathcal{S} = (V, E, F)$ with vertices $\mathbf{v}_i = (x_i, y_i, s_i)$ can be put into static equilibrium with vertical forces "$A_i F_i$" if and only if there exists a combinatorially equivalent mesh Φ with planar faces and vertices (x_i, y_i, ϕ_i), such that curvatures of $\mathcal{S}$ relative to Φ obey*

$$2K_\Phi(\mathbf{v}_i) H^{\text{rel}}(\mathbf{v}_i) = F_i \qquad (7)$$

at every interior vertex and every free boundary vertex $\mathbf{v}_i$. $\mathcal{S}$ can be put into compressive static equilibrium if and only if there exists a convex such Φ.

Proof. The relation between equilibrium forces $w_{ij} \mathbf{e}_{ij}$ in $\mathcal{S}$ and the polyhedral stress potential Φ has been discussed above, and so has the equivalence "$w_{ij} \geq 0 \iff \Phi$ convex" (see e.g. [Ash et al. 1988] for a survey of this and related results). It remains to show that Equations (2) and (7) are equivalent. This is the case because the proposition above implies $2K(\mathbf{v}_i) H^{\text{rel}}(\mathbf{v}_i) = 2 \frac{A_i(\Phi, \Phi)}{A_i} \frac{A_i(\Phi, \mathcal{S})}{A_i(\Phi, \Phi)} = \frac{1}{A_i} (\sum_{j \sim i} w_{ij}(s_j - s_i)) = \frac{1}{A_i} A_i F_i$. $\qquad \square$

Relation to discrete Laplace-Beltrami operators. For a given smooth surface $\mathcal{S}$ with Airy stress function ϕ, and a given discrete top view $\mathcal{R}'$, does there exist a polyhedral surface $\mathcal{R}$ in equilibrium approximating $\mathcal{S}$? We restrict our attention to triangle meshes, where planarity of the faces of the discrete stress surface Φ is not an issue.

This question has several equivalent reformulations:

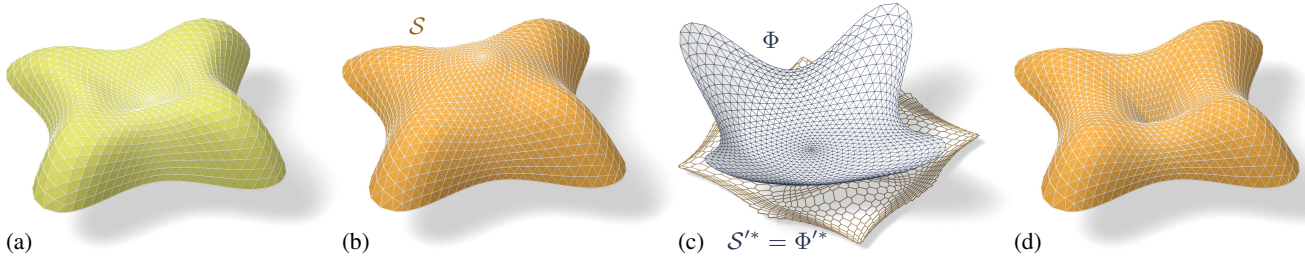- Does $\mathcal{R}'$ have a reciprocal diagram whose polar dual approximates ϕ?

Figure 6: *The top of the Lilium Tower (a) cannot stand as a masonry structure. (b) Our algorithm finds a nearby self-supporting mesh without this impossible feature. (c) shows the corresponding Airy mesh Φ and reciprocal force diagram $\mathcal{S}'^*$. (d) The user can edit the original surface, such as by specifying that the center of the surface is supported by a vertical pillar, and the self-supporting network adjusts accordingly*

- Does $\mathcal{R}'$ possess a "perfect" discrete Laplace-Beltrami operator Δ_ϕ (in the sense of Wardetzky et al. [2007]) whose weights are the edge length scalars of such a reciprocal diagram?

It is known [Wardetzky et al. 2007] that even in the special case of $\phi = \phi_0$ the answer is not always affirmative, unless $\mathcal{R}'$ is a Delaunay triangulation. From the previous sections, we can state a sufficient condition for general ϕ: if $\mathcal{R}'$ lifts to a (strictly) convex polyhedron Φ with vertices on ϕ, its polar dual is a reciprocal diagram with positive edge weights, Δ_ϕ has positive weights, and $\mathcal{R}$, given by the solution of the discrete Poisson problem on $\mathcal{R}'$, approximates $\mathcal{S}$. Moreover, every top view for every ϕ can be retriangulated in a way that Φ is convex, by lifting the top view to ϕ and taking the convex hull. Since ϕ is convex, every vertex lies on the boundary of the convex hull, and faces of the convex hull give the faces of a retriangulation of $\mathcal{R}'$ for which Φ is convex. Equivalently, every mesh $\mathcal{R}'$ admits a Delaunay-like triangulation for which a "perfect" generalized Laplacian Δ_ϕ exists.

Therefore, while the choice of edges in $\mathcal{R}'$ is important, the choice of vertices is not: a smooth self-supporting surface can be approximated by a discrete self-supporting triangular mesh for any sampling of the surface.

3 Thrust Networks from Reference Meshes

Consider now the problem of taking a given reference mesh, $\mathcal{R}$ and finding a combinatorially equivalent mesh $\mathcal{S}$ in static equilibrium approximating $\mathcal{R}$. The loads on $\mathcal{S}$ include user-prescribed loads as well as the dead load caused by the mesh's own weight (which depends on the vertices $\mathbf{v}_i$ of $\mathcal{S}$.) Conceptually, finding $\mathcal{S}$ amounts to minimizing some formulation of distance between $\mathcal{R}$ and $\mathcal{S}$, subject to constraints (2), (3), and $w_{ij} \geq 0$. For any choice of distance this minimization will be a nonlinear, non-convex, inequality-constrained variational problem that cannot be efficiently solved in practice. Instead we propose a staggered optimization algorithm:

1. Start with an initial guess $\mathcal{S} = \mathcal{R}$.
2. Estimate the self-load on the vertices of $\mathcal{S}$ from their current positions.
3. Fixing $\mathcal{S}$, try to fit an associated stress surface Φ.
4. Alter positions $\mathbf{v}_i$ to improve the fit.
5. Repeat from step 2 until convergence.

Estimating Self-load. Since we need to include the self-weight of the surface as a component of the load on $\mathcal{S}$, F_i depends not only on the top view of $\mathcal{S}$ but also on the surface area of its faces. To avoid adding nonlinearity to the algorithm, we estimate F_i at the beginning of each iteration, and assume it remains constant until the next iteration. We estimate the mass at each vertex by calculating

its Voronoi area on each of its incident faces, and then multiplying by a user-specified surface density ρ.

Fit a Stress Surface. In this step, we fix $\mathcal{S}$ and try to fit a stress surface Φ subordinate to the top view $\mathcal{S}'$ of the primal mesh. We do so by searching for convex face normals for Φ which minimize, in the least-squares sense, the error in force equilibrium (7) and local integrability of Φ. Doing so is equivalent to minimizing the squared residuals of equations (3) and (2), respectively, with the positions held fixed:

$$\min_{w_{ij}} \sum_i \left\| \begin{pmatrix} 0 \\ 0 \\ A_i F_i \end{pmatrix} - \sum_{j \sim i} w_{ij}(\mathbf{v}_j - \mathbf{v}_i) \right\|^2$$
$$\text{s.t. } 0 \leq w_{ij} \leq w_{\max}, \qquad (8)$$

where the outer sum is over the interior and free boundary vertices, and $w_{\max}$ is an optional maximum weight we are willing to assign (to limit the amount of stress in the surface). This convex, sparse, box-constrained least-squares [Friedlander 2007] problem always has a solution. If the objective is 0 at this solution, the faces of Φ locally integrate to a stress surface satisfying (7), and so Φ certifies that $\mathcal{S}$ is self-supporting – we are done. Otherwise, $\mathcal{S}$ is not self-supporting and its vertices must be moved.

Alter Positions. In the previous step we fit as best as possible a stress surface Φ to $\mathcal{S}$. There are two possible kinds of error with this fit: the faces around a vertex (equivalently, the reciprocal diagram) might not close up; and the resulting stress forces might not be exactly in equilibrium with the loads. These errors can be decreased by modifying the top view and heights of $\mathcal{S}$, respectively. It is possible to simply solve for new vertex positions that put $\mathcal{S}$ in static equilibrium, since equations (2) and (3) with w_{ij} fixed form a square linear system that is typically nonsingular.

While this approach would yield a self-supporting $\mathcal{S}$, this mesh is often far from the reference mesh $\mathcal{R}$, since any local errors in the stress surface from step 3 amplify into global errors in $\mathcal{S}$. We propose instead to look for new positions that decrease the imbalance in the stresses and loads, while also penalizing drift away from the reference mesh:

$$\min_{\mathbf{v}} \sum_i \left\| \begin{pmatrix} 0 \\ 0 \\ A_i F_i \end{pmatrix} - \sum_{j \sim i} w_{ij}(\mathbf{v}_j - \mathbf{v}_i) \right\|^2$$
$$+ \alpha \sum_i \langle \mathbf{n}_i, \mathbf{v}_i - \mathbf{v}_i^0 \rangle^2 + \beta \|\mathbf{v} - \mathbf{v}_P^0\|^2,$$

where $\mathbf{v}_i^0$ is the position of the i-th vertex at the start of this step of the optimization, $\mathbf{n}_i$ is the starting vertex normal (computed as the average of the incident face normals), $\mathbf{v}_P^0$ is the projection of $\mathbf{v}^0$ onto the reference mesh, and $\alpha > \beta$ are penalty coefficients that are
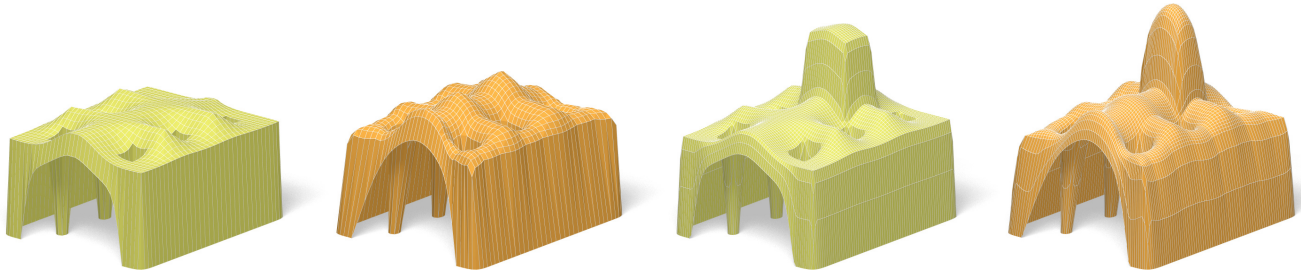
Figure 7: *The user-designed reference mesh (left) is not self-supporting, but our algorithm finds a nearby perturbation of the reference surface (middle-left) that is in equilibrium. As the user makes edits to the reference surface (middle-right), the thrust network automatically adjusts (right).*

decreased every iteration of steps 2-4 of the algorithm. The second term allows $\mathcal{S}$ to slide over itself (if doing so improves equilibrium) but penalizes drift in the normal direction. The third term, weaker than the second, regularizes the optimization by preventing large drift away from the reference surface or excessive tangential sliding.

Geometric interpretation of this step. It is *almost* fixing the dihedral angles of the stress surface, and adjusting the top view to improve the integrability of the stress surface – this would be the case if the edges of the top view were constrained to have fixed lengths. (We don't want to do this, of course, since that would make the top view uselessly rigid (not to mention make the optimization non-linear.) I need to reflect more on this.

Solving this weighted least-squares problem amounts to solving a sparse, symmetric linear system. While the MINRES algorithm [Paige and Saunders 1975] is likely the most robust algorithm for solving this system, in practice we have observed that the method of conjugate gradients works well despite the potential ill-conditioning of the objective matrix.

Convergence. This algorithm is not guaranteed to always converge; this fact is not surprising from the physics of the problem (if the boundary of the reference mesh encloses too large of a region, w_{max} is set too low, and the density of the surface too high, a thrust network in equilibrium simply does not exist – the vault is too ambitious and cannot be built to stand; pillars are needed.) We can, however, make a few remarks. Step 3 always decreases the equilibrium energy

$$E = \sum_i \left\| \begin{pmatrix} 0 \\ 0 \\ A_i F_i \end{pmatrix} - \sum_{j \sim i} w_{ij}(\mathbf{v}_j - \mathbf{v}_i) \right\|^2$$

and step 4 does as well as $\beta \to 0$. Moreover, as $\alpha \to 0$ and $\beta \to 0$, step 4 approaches a linear system with as many equations as unknowns; if this system has full rank, its solution sets $E = 0$. These facts suggest that the algorithm should generally converge to a thrust network in equilibrium, provided that step 2 does not increase the loads by too much at every iteration, and this is indeed what we observe in practice. It would be nice if I could prove that, for sufficiently large w_{max}, step 2 cannot cause the algorithm to fail to converge, but I don't yet know how to approach this problem.

If the linear system in step 4 is singular and infeasible, the algorithm can stall at $E > 0$. This failure occurs, for instance, when an interior vertex has height z_i lower than all of its neighbors, and step 3 assigns all incident edges to that vertex a weight of zero: clearly no amount of moving the vertex or its neighbors can bring the vertex into equilibrium. We avoid such degenerate configurations by bounding weights slightly away from zero in (8), trading increased robustness for slight smoothing of the resulting surface.

4 Design of Self-Supporting Surface

The optimization algorithm described in the previous section forms the basis of an interactive design tool for self-supporting surfaces. Users manipulate a mesh representing a reference surface, and the computer searches for a nearby thrust network in equilibrium. Fitting this thrust network does not require that the user specify boundary tractions, and although the top view of the reference mesh is used as an initial guess for the top view of the thrust network, the search is not restricted to this top view.

Some features of the design tool include:

- Handle-based 3D editing of the reference mesh using Laplacian coordinates [Lipman et al. 2004; Sorkine et al. 2003] to extrude vaults, insert pillars, and apply other deformations to the reference mesh. Handle-based adjustments of the heights, keeping the top view fixed, and deformation of the top view, keeping the heights fixed, are also supported. The thrust network adjusts interactively to fit the deformed positions, giving the usual visual feedback about the effects of her edits on whether or not the surface can stand.

- Specification of boundary conditions. Points of contact between the reference surface and the ground or environment are specified by "pinning" vertices of the surface, specifying that the thrust network must coincide with the reference mesh at this point, and relaxing the condition that forces must be in equilibrium there.

- Interactive adjustment of surface density ρ, external loads, and maximum permissible stress per edge w_{max}, with visual feedback of how these parameters affect the fitted thrust network.

- Upsampling of the thrust network through Catmull-Clark subdivision [**?**] and polishing of the resulting refined thrust network using optimization (§3).

- Visualization of the stress surface R dual to the thrust network.

TODO more to come?

Vault with Pillars. As an example of the design and optimization workflow, consider a rectangular vault with six pillars, free boundary conditions along one edge, fixed boundary conditions along the others, and a tower extruded from the top of the surface (see Figure 7). This surface is non-convex, non-simply-connected, and exhibits a mix of boundary conditions, none of which cause our algorithm any difficulty; it finds a self-supporting thrust network near the designed reference mesh. The user is now free to make edits to the ref-

erence mesh, and the thrust network adapts to these edits, providing the user feedback on whether her designs are physically realizable.

Top of the Lilium Tower. Consider the top portion of the steel-glass exterior surface of the Lilium Tower (see Figure 6). This surface contains a local minimum in its interior and so cannot possibly be self-supporting; more generally, the entire central portion of the surface has positive Gaussian curvature and points downwards, an impossible feature in a self-supporting mesh. Given this surface as a reference mesh, our algorithm constructs a nearby thrust network in equilibrium without the impossible feature. The user can then explore how editing the reference mesh – adding a pillar, for example – affects the thrust network and its deviation from the reference surface.

5 Special Families of Self-Supporting Surfaces

PQ Meshes. Meshes with *planar* faces are of particular interest in architecture, so in this section we discuss how to remesh a given thrust network in equilibrium such that it becomes a quad mesh with planar faces (again in equilibrium). For this purpose we first demonstrate how to find a quad mesh $\mathcal{S}$ with vertices $\mathbf{v}_{ij} = (x_{ij}, y_{ij}, s_{ij})$ which approximates a given continuous surface $s(x, y)$ equipped with an equilibrium stress potential $\phi(x, y)$.

It is known that $\mathcal{S}$ must approximately follow a network of conjugate curves in the surface (see e.g. [Liu et al. 2006]). We can derive this condition in an elementary way as follows: Using a Taylor expansion, we compute the volume of the convex hull of the quadrilateral $\mathbf{v}_{ij}, \mathbf{v}_{i+1,j}, \mathbf{v}_{i+1,j+1}, \mathbf{v}_{i,j+1}$, assuming the vertices lie exactly on the surface $s(x, y)$. This results in

$$\text{vol} = \tfrac{1}{6} \det(\mathbf{a}_1, \mathbf{a}_2, (\mathbf{a}_1)^T \nabla^2 s \, \mathbf{a}_2) + \cdots ,$$

$$\text{where } \mathbf{a}_1 = \begin{pmatrix} x_{i+1,j} - x_{ij} \\ y_{i+1,j} - y_{ij} \end{pmatrix}, \quad \mathbf{a}_2 = \begin{pmatrix} x_{i,j+1} - x_{ij} \\ y_{i,j+1} - y_{ij} \end{pmatrix},$$

and the dots indicate higher order terms. We see that planarity requires $(\mathbf{a}_1)^T \nabla^2 s \, \mathbf{a}_2 = 0$. In addition to the mesh $\mathcal{S}$ approximating the surface $s(x, y)$, the corresponding polyhedral Airy surface Φ must approximate $\phi(x, y)$; thus we get the conditions

$$(\mathbf{a}_1)^T \nabla^2 s \, \mathbf{a}_2 = (\mathbf{a}_1)^T \nabla^2 \phi \, \mathbf{a}_2 = 0.$$

$\mathbf{a}_1, \mathbf{a}_2$ are therefore eigenvectors of $(\nabla^2 \phi)^{-1} \nabla^2 s$. In view of §2.3, $\mathbf{a}_1, \mathbf{a}_2$ indicate the principal directions of the surface $s(x, y)$ relative to $\phi(x, y)$ (see Figure 8).
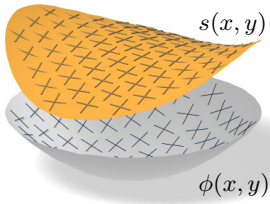
Figure 8: *A planar quad mesh approximating a self-supporting surface $s(x, y)$ with stress potential $\phi(x, y)$ is guided by the principal curvature directions of s relative to ϕ (found from eigenvectors of $(\nabla^2 \phi)^{-1} \nabla^2 s$.)*

In the discrete case, where s, ϕ are not given as continuous surfaces, but are represented by a mesh in equilibrium and its Airy mesh, we use the techniques of Schiftner [2007] and Cohen-Steiner and Morvan [2003] to approximate the Hessians $\nabla^2 s$, $\nabla^2 \phi$, compute principal directions as eigenvectors of $(\nabla^2 \phi)^{-1} \nabla^2 s$, and subsequently find meshes $\mathcal{S}, \Phi$ approximating s, ϕ which follow those directions. Subseqent global optimization makes $\mathcal{S}, \Phi$ a valid thrust network with discrete stress potential. Convexity of Φ ensures that $\mathcal{S}$ is self-supporting.
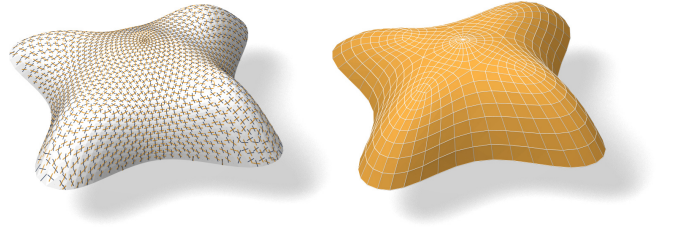
Figure 9: *Integrating the principal relative curvature directions of a surface in equilibrium yields a self-supporting, planar quad remeshing of that surface (right).*

Figure 9 illustrates the result of applying this procedure to a self-supporting modification of the Lilium tower. TODO more examples

Koenigs Meshes. Consider a self-supporting thrust network $\mathcal{S}$ and corresponding Airy mesh Φ. Both $\mathcal{S}$ and Φ are elements of the linear space of meshes which project onto $\mathcal{S}'$. Any such mesh has vertices $\mathbf{v}_i = (x_i, y_i, z_i)$, where the choice $z_i = s_i$ leads to $\mathcal{S}$ and $z_i = \phi_i$ leads to Φ. We already know that the vertical loads $A_i F_i$ which put $\mathcal{S}$ into equilibrium are computed as $AF = \Delta_\phi s$.

Which perturbations $\mathcal{S} + \mathcal{R}$, having z coordinates $z_i = s_i + r_i$, support the *same* vertical loads as $\mathcal{S}$ does? Such a mesh must satisfy $\Delta_\phi(s + r) = \Delta_\phi s$, so $\Delta_\phi r = 0$, i.e., r is a harmonic function. Such harmonic functions are easily computed, given any boundary conditions.

However there is a very nice explicit geometric construction of all harmonic functions in the case of quad meshes: Equation (7) immediately leads to $H_{\mathcal{S}}^{\text{rel}} = H_{\mathcal{S}+\mathcal{R}}^{\text{rel}}$, which is equivalent to

$$H_{\mathcal{R}}^{\text{rel}} = 0.$$

So $\mathcal{R}$ is a *minimal surface*. Recall that $H_{\mathcal{R}}^{\text{rel}}$ is the mean curvature of $\mathcal{R}^*$ with respect to the Gauss image Φ^* in the sense of [Pottmann et al. 2007], where the star indicates the polar polyhedron. We conclude that $\mathcal{R}^*$ is constructed from Φ^* by the condition of *parallel non-corresponding diagonals*, which is also called Christoffel duality, and which can be seen in Figure 5. This condition determines $\mathcal{R}^*$ uniquely up to translation and scaling; thus $\mathcal{R}$ is unique up to scaling of z coordinates and adding linear functions.

A particularly interesting special case are *isotropic Koebe meshes* – PQ meshes $\mathcal{S}$ whose edges are tangent to the Maxwell paraboloid ϕ_0. Such meshes, by approximating the isotropic sphere, satisfy $2K(\mathbf{v}_i)H^{rel}(\mathbf{v}_i) \approx 1$ and so, if their load density over the plane is constant, are very close to self-supporting. Since the intersection of a paraboloid with a sphere forms a circle, each face of $\mathcal{S}$ contains an inscribed circle, as does its corresponding minimal surface $\mathcal{R}$ (since polar and Chistoffel duality preserve this property [Pottmann
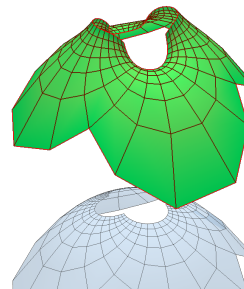
Figure 10: *From a self-supporting isotropic Koebe surface, it is possible to construct a family of new self-supporting meshes, with identical top view, using the Christoffel construction.*

and Liu 2007]), and all PQ, self-supporting combinations $\mathcal{S} + \alpha\mathcal{R}$. Figure 10 shows one example of such an $\mathcal{S}$ and $\mathcal{S} + \alpha\mathcal{R}$.

6 Conclusion and Future Work

TODO Some ideas:

- Non-manifold surfaces
- Non-vertical loads
- Adaptive remeshing

References

ASH, P., BOLKER, E., CRAPO, H., AND WHITELEY, W. 1988. Convex polyhedra, Dirichlet tessellations, and spider webs. In *Shaping space (Northampton, Mass., 1984)*. Birkhäuser, Boston, 231–250.

BARNES, M. R. 2009. Form finding and analysis of tension structures by dynamic relaxation. *International Journal of Space Structures 14*, 2, 89–104.

BLOCK, P., AND LACHAUER, L. 2011. Closest-fit, compression-only solutions for free form shells. In *IABSE — IASS 2011 London Symposium*, Int. Ass. Shell Spatial Structures. electronic, 8 pp.

BLOCK, P., AND OCHSENDORF, J. 2007. Thrust network analysis: A new methodology for three-dimensional equilibrium. *J. Int. Assoc. Shell and Spatial Structures 48*, 3, 167–173.

COHEN-STEINER, D., AND MORVAN, J.-M. 2003. Restricted Delaunay triangulations and normal cycle. In *Proc. 19th Symp. Computational geometry*, ACM, 312–321.

FRATERNALI, F., ANGELILLO, M., AND FORTUNATO, A. 2002. A lumped stress method for plane elastic problems and the discrete-continuum approximation. *Int. J. Solids Struct. 39*, 6211–6240.

FRATERNALI, F. 2010. A thrust network approach to the equilibrium problem of unreinforced masonry vaults via polyhedral stress functions. *Mechanics Res. Comm. 37*, 2, 198 – 204.

FRIEDLANDER, M. P., 2007. BCLS: Bound constrained least squares. *http://www.cs.ubc.ca/~mpf/bcls*.

GIAQUINTA, M., AND GIUSTI, E. 1985. Researches on the equilibrium of masonry structures. *Archive for Rational Mechanics and Analysis 88*, 4, 359–392.

GLYMPH, J., SHELDEN, D., CECCATO, C., MUSSEL, J., AND SCHOBER, H. 2004. A parametric strategy for free-form glass structures using quadrilateral planar facets. *Automation in Construction 13*, 2, 187 – 202.

HEYMAN, J. 1966. The stone skeleton. *Int. J. Solids Structures 2*, 249–279.

HEYMAN, J. 1995. *The Stone Skeleton: Structural Engineering of Masonry Architecture*. Cambridge University Press.

HEYMAN, J. 1998. *Structural Analysis: A Historical Approach*. Cambridge University Press.

KILIAN, A., AND OCHSENDORF, J. 2005. Particle-spring systems for structural form finding. *J. Int. Assoc. Shell and Spatial Structures 46*, 77–84.

LIPMAN, Y., SORKINE, O., COHEN-OR, D., LEVIN, D., ROSSI, C., AND SEIDEL, H. 2004. Differential coordinates for interactive mesh editing. In *Proc. SMI*. IEEE, 181–190.

LIU, Y., POTTMANN, H., WALLNER, J., YANG, Y.-L., AND WANG, W. 2006. Geometric modeling with conical meshes and developable surfaces. *ACM Trans. Graph. 25*, 3, 681–689.

LIVESLEY, R. K. 1992. A computational model for the limit analysis of three-dimensional masonry structures. *Meccanica 27*, 161–172.

O'DWYER, D. 1998. Funicular analysis of masonry vaults. *Computers and Structures 73*, 187–197.

PAIGE, C. C., AND SAUNDERS, M. A. 1975. Solution of sparse indefinite systems of linear equations. *SIAM Journal on Numerical Analysis 12*, 617–629.

POTTMANN, H., AND LIU, Y. 2007. Discrete surfaces in isotropic geometry. In *Mathematics of Surfaces XII*, M. Sabin and J. Winkler, Eds. Springer-Verlag, 341–363.

POTTMANN, H., LIU, Y., WALLNER, J., BOBENKO, A., AND WANG, W. 2007. Geometry of multi-layer freeform structures for architecture. *ACM Trans. Graphics 26*, 3, #65,1–11.

SCHEK, H.-J. 1974. The force density method for form finding and computation of general networks. *Computer Methods in Applied Mathematics and Engineering 3*, 115–134.

SCHIFTNER, A., AND BALZER, J. 2010. Statics-sensitive layout of planar quadrilateral meshes. In *Advances in Architectural Geometry 2010*, C. Ceccato et al., Eds. Springer, Vienna, 221–236.

SCHIFTNER, A. 2007. *Planar quad meshes from relative principal curvature lines*. Master's thesis, TU Wien.

SORKINE, O., COHEN-OR, D., AND TOLEDO, S. 2003. High-pass quantization for mesh encoding. In *Symposium Geometry processing*. 42–51.

VAN MELE, T., AND BLOCK, P. 2011. A novel form finding method for fabric formwork for concrete shells. *J. Int. Assoc. Shell and Spatial Structures 52*, 217–224.

WARDETZKY, M., MATHUR, S., KÄLBERER, F., AND GRINSPUN, E. 2007. Discrete Laplace operators: No free lunch. In *Symposium on Geometry Processing*. 33–37.

WHITING, E., OCHSENDORF, J., AND DURAND, F. 2009. Procedural modeling of structurally-sound masonry buildings. *ACM Trans. Graph. 28*, 5, #112,1–9.